

On the Isovector Form Factors of the Nucleon in Meson Theory

Fritz Gutbrod and Guido Hartmann

Deutsches Elektronen-Synchrotron DESY, D-2000 Hamburg, Federal Republic of Germany

Received 25 January 1979

Abstract. We present a calculation of the nucleon isovector form factors for low momentum transfer. Our model is based on skeleton diagrams in pseudo-scalar πN interaction where unknown parameters describing higher order corrections are fixed such that a ρ meson is generated dynamically with the correct properties. The normalization of the form factors and the radii agree well with experiment. For $-q^2$ up to 1 GeV^2 the contributions of the $\pi\omega$ -intermediate state do not fall off rapidly enough to give perfect agreement with the dipole formulae.

1. Introduction

The electromagnetic form factors of the nucleon contain highly valuable information on the dynamics of strong interactions, and any model for hadrons should be confronted with the accurate experimental data [1]. Unfortunately our understanding of the nucleon structure is rather poor and the general rules for an interpretation of the observations are unclear. There is consensus that the nucleon is a highly composite object, but it is an open question what kind of constituents are needed to describe its spatial extension. Is it reasonable, at least for moderate q^2 -values, to imagine the nucleon as being composed of itself and a certain number of mesons, similarly as one describes the extension of the electron in QED, or is its e.m. structure the manifestation of a wave function of three pointlike quarks? Or are also the quarks extended objects (especially via their coupling to vector mesons), so that we see the convolution of a wave function and the constituent's extension, similarly to the situation for light nuclei? It would be natural to guess a ρ -pole behaviour for the quark form factor. If so, what is the wave function radius of the pion, the form factor of which is to a good approximation dominated by the ρ -pole [2]?

In this paper we work out a consistent field theoretic picture for the nucleon isovector form factors in the framework, where the nucleon is assumed to be

composed of itself and of mesons. We shall calculate $F_1(q^2)$ and $F_2(q^2)$ in the range $0 \leq -q^2 \leq 1 \text{ GeV}^2/c^2$ in various approximations. The simplest one is shown in Fig. 1a, which describes the one-nucleon exchange part of the meson current with the photon meson coupling taken as the full, renormalized vertex. (The distinction between meson and nucleon currents in higher order perturbation theory is a matter of definition. For a meson current we adopt the criterium of two meson reducibility starting from the side of the outgoing nucleons. Thus also the diagram of Fig. 1b is called a meson current, although it could be regarded as a nucleon current as shown in Fig. 1c). We shall see that the meson current Fig. 1a gives large contributions to both form factors and that its q^2 -behaviour is already quite characteristic for the final result of the model, especially for $F_2(q^2)$. Since at least the on-shell pion radius is not much smaller than the nucleon radius (0.6 fm as compared to 0.8 fm), we need for the pion current a small radius of the "wave function" between the extended pion and the nucleon. This can qualitatively be expected [3] as the result of the standard pseudoscalar πN -interaction which becomes really strong only at momenta of the order of the nucleon mass. That the interaction of

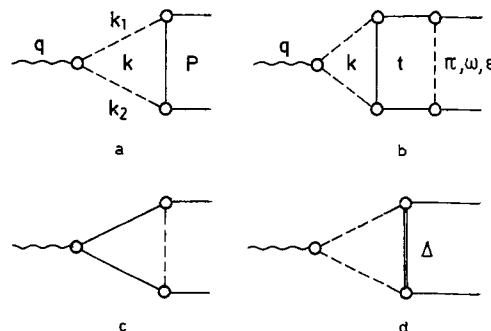


Fig. 1. a Nucleon exchange diagram for the pion current, b box diagram for the pion current. The exchanged mesons are indicated, c nucleon current diagram, d Δ -exchange diagram

the constituents is of short range and that the apparent size of the nucleon is largely caused by the low masses of the intermediate vector mesons seems to be an appealing picture in view of the recent observation [4] that the transverse momenta of directly produced hadrons and μ -pairs in pp -collisions are not much smaller than 1 GeV/c.

The description of an extended pion in a field theoretic calculation is far from trivial. Although we have shown [5,6] that the coupling between $\pi\pi$, $\pi\omega$ and $N\bar{N}$ states via N -exchange dynamically creates a ρ -meson, this ρ a priori need not dominate the e.m. pion vertex, especially if the pions are off-shell. Our model works very well in this respect. It will turn out that the off-shell pion form factor indeed decreases less rapidly with q^2 than on-shell, but for the nucleon form factors this is compensated by the wave function effects. In diagrammatic language these effects are a combination of the strong vertex functions and the propagators in Fig. 1a. These quantities are already fixed by our model for the ρ -meson. There we assume a specific form of the πN vertex, and the scale parameter of this function is adjusted to obtain the correct ρ mass. Then the pion e.m. vertex and from it the pion propagator are determined without further parameters. The calculation of the nucleon propagator is much more complicated because of spin effects, and we rely on recent work by one of us [7]. Thus we can treat all Feynman diagrams as skeleton diagrams with dressed vertices and propagators. Whether the perturbation expansion for the Bethe-Salpeter kernel, which we need for the ρ -meson, is convergent in terms of skeleton diagrams is of course completely open. We hope that large classes of poorly converging diagrams can be absorbed into resonance exchanges like ω -exchange etc.

Since we claim that the $N\bar{N}$ intermediate state is crucial for understanding the ρ -meson, we must correctly account for the couplings of the ρ to $N\bar{N}$. These couplings manifest themselves in the normalization of the form factors and in their derivatives with respect to q^2 . Considering first the charge normalization, $F_1(0)$, this is finite for the diagram of Fig. 1a, since our pion vertex will acquire a powerlike decrease for spacelike momenta. The nucleon exchange contribution will have almost twice the correct value. This is consistent with the fact that Δ -exchange and π -exchange between $N\bar{N}$ (Fig. 1d and 1b resp.) give negative charge contributions. Already in [6] we used a reduction of the $\pi\pi - N\bar{N}$ amplitude due to pion exchange. With respect to $F_2(0)$ it is well known [8] that the diagrams Figs. 1a and 1c with pointlike vertices and free propagators give a good value for the isovector anomalous magnetic moment. By dressing the vertices and propagators the moment will be reduced considerably, so that higher order contributions are necessary to compensate this effect. Possible candidates are the $\pi\omega$ -current, Fig. 2, Δ -exchange Fig. 1d and ω and ε -exchange Fig. 1b.

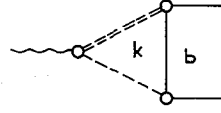


Fig. 2. $\pi\omega$ -current

Altogether these diagrams give the normalization for $F_1(0)$ and $F_2(0)$ within 10%.

The e.m. radii agree with experiment within 10% for all approximations except the simplest one, Fig. 1a, for $F_1(q^2)$ which is much too low. There the long tail in momentum space of the vertex diagram is still important. The full model can account for $F_1(q^2)$ perfectly, whereas the $\pi\omega$ -current leads to certain problems for $F_2(q^2)$ at the upper end of our q^2 -interval. The main source of this trouble is the $\pi\omega$ form factor $F_{\pi\omega\gamma}$ itself, which falls off more slowly than vector dominance in our model. This question will have to be studied by $\pi\omega$ production in the timelike region.

In section 2 we review our model for the ρ -meson and the pion form factor and discuss some modifications relative to [6]. In section 3 we calculate the various pion current contributions, namely N - and Δ -exchange and the box diagrams of Fig. 1b. Section 4 deals with the $\pi\omega$ -current, and in Sect. 5 we recapitulate our results and draw conclusions.

2. The Pion Form Factor

The theory for the e.m. off-shell pion vertex $F_\pi(q, k)$ (see Fig. 1a for kinematics) in our q^2 -region is essentially a theory for the ρ -meson. We assume [5,6] that $N\bar{N}$ interact predominantly via the annihilation into $\pi\pi$, $K\bar{K}$ and $\pi\omega$ states by N -exchange. In order to incorporate higher order effects we work with dressed vertices and propagators. Especially we parametrize the pseudoscalar πN -vertex function by the following ansatz (see Fig. 3 for momenta)

$$\gamma_5 \Gamma_5(p_1^2, p_2^2, p_3^2) = \gamma_5 \left(1 - \sum_{i=1}^3 (p_i^2 - m_i^2) / \Lambda^2 \right) \quad (2.1)$$

where the scale parameter Λ will be fixed by the ρ -mass. The ρ is found as a $\pi\pi$ resonance in the solution of the multichannel Bethe-Salpeter equation. The coupling between the $N\bar{N}$ and the $\pi\omega$ channel is determined by the vector coupling constant $g_{\omega N\bar{N}}$, which is adjusted to fit the decay $\omega \rightarrow \pi_0 \gamma$. The pion and nucleon propagators are those found by an application of the Ward identity in [6, 7]. In principle the model predicts the ρ -width. As it is natural for a

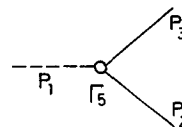


Fig. 3. Definition of momenta for $\pi N\bar{N}$ -vertex

few channel approximation to the real world, the coupling to the channels considered will be overestimated, and consequently we have difficulties to reproduce the low value of $\Gamma_\rho = 150$ MeV. We therefore tried to correct the deficiencies of our model by three modifications compared to [6] (quoted as GW henceforth):

2.1. Modification of the Nucleon Box

In GW we speculated that the repulsive pion exchange between $N\bar{N}$ would reduce the nucleon box diagram for $\pi\pi \rightarrow \pi\pi$ by about 35%. In appendix A we have set up a simplified BSE for $N\bar{N}$ scattering where one sees that the reduction is about 20%. Furthermore the inclusion of other meson exchanges cancels this effect. However, one obtains a stronger q^2 -dependence as compared to the “empty” box, namely an increase of 9% from $q^2 = 0$ to $q^2 = m_\rho^2$. These rough calculations agree qualitatively with the full solutions of the BSE in [9]. With these changes in the loop we find (including other corrections explained below) the width $\Gamma_\rho = 173$ MeV. In order to achieve the correct value we choose a reduction factor of 0.8 and a stronger q^2 -dependence. This may be justified by the presence of other repulsive forces like Δ -exchange.

2.2. Modification of the Pion Propagator

Our strong vertex function (2.1) acts as a cut-off in momentum space, and it has to be checked whether our model still respects unitarity of scattering amplitudes. Of course the introduction of an effective πN -vertex function is perfectly legitimate as it represents the sum of vertex diagrams. It must however be accompanied by higher order meson production processes, since otherwise unitarity in the perturbative sense will be violated. Part of these production diagrams are contained in the dressed propagators but one can give qualitative arguments that this is not sufficient.

Let us consider the $N\bar{N}$ scattering amplitude in the quantum number state of the pion as a function of the squared CM-energy σ . The amplitude has a pole at $\sigma = m_\pi^2$ and, from unitarity, a positive imaginary continuum starting at $\sigma = 9m_\pi^2$. The $N\bar{N}$ amplitude also has a “left hand” singularity, the beginning of which, σ_L , depends on the exchanged and the external masses, which we treat as variable. The sign of the left hand cut contribution is model dependent, but in potential theory for attractive potentials it is positive for $\sigma > \sigma_L$, and it interferes destructively with the right hand cut for $\sigma \rightarrow \pm\infty$. Therefore in the interval $\sigma_L < \sigma < m_\pi^2$ the amplitude must exceed the pion pole contribution. We assume this property to hold also for off-shell nucleons which occur in our annihilation diagrams. For simplicity we consider only equal momenta squared p^2 for these

nucleons. Then the left hand cut starts at

$$\sigma_L(p^2) = 4p^2 - m_t^2 \quad (2.2)$$

where m_t is the smallest exchanged mass. For this we take the average between scattering diagrams ($m_t^2 = 4m_\pi^2$) and annihilation diagrams ($m_t^2 = 4M^2$, $M =$ nucleon mass). We now simply add a pole term to the renormalized pion propagator $\tilde{A}(\sigma)$,

$$A_{\text{eff}}(\sigma) = \tilde{A}(\sigma) + c/(\sigma - M_1^2) \quad (2.3)$$

where M_1 is a typical multiparticle mass. We take $M_1^2 = 3M^2$. The constant c is then adjusted such that there is no unitarity violation in the range $0 > p^2 > -M^2$, which is representative for the box diagram. This means

$$\Gamma_5^2(p^2, p^2, \sigma) A_{\text{eff}}(\sigma) \geq \Gamma_5^2(p^2, p^2, m_\pi^2)/(\sigma - m_\pi^2) \quad (2.4)$$

for $\sigma > \sigma_L(p^2)$. We find $c = 0.6$, which changes $\tilde{A}(\sigma)$ by less than 15%. The smallness of this correction is a consequence of dressing the meson propagator.

2.3. The ω -Propagator

In GW the scalar part of the ω -propagator was taken, after shifting the mass, equal to the pion propagator. From [9] we know that to a good approximation the ω can be described as a bound $N\bar{N}$ -system with π -exchange as the dominant force. This allows us to define the product of two $\omega N\bar{N}$ vertex functions and the ω -propagator as the sum of $N\bar{N}$ scattering diagrams with π -exchange. It should be noted however that single π -exchange has to be left out from this sum, since it is equivalent, if inserted for the $\pi\omega$ -intermediate state, to single π -exchange with a vertex correction. There is also some double counting for two-pion exchange, as it is part of scalar meson exchange within the nucleon box. In the simplified BSE for $N\bar{N}$ scattering described in appendix A we have analyzed the scattering diagrams as functions of energy and off-shell momenta. Especially the sum without the first two terms can very well be represented by the free propagator, with a vertex function dropping off slightly faster in p^2 than (2.1). The coupling constant $g_{\omega N\bar{N}/4\pi}^2$ is around 15 (see Fig. 8).

The use of the free ω -propagator instead of the dressed one will increase the ρ -width as compared to GW. This is the reason why we had to introduce the previous two corrections. We remark that none of these corrections is very large and that they are necessary to improve some of the deficiencies inherent in a model with few annihilation channels.

2.4. The Pion Form Factor

The value of the vertex scale parameter is now $1.73 \text{ GeV}^2/c^2$. The pion form factor resulting from our model is shown in Fig. 4 in comparison with experimental data [2] in the spacelike region. Obviously the deviations from simple VDM are

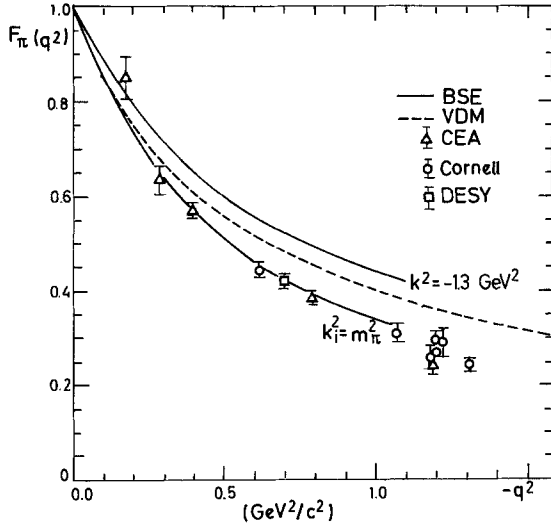


Fig. 4. Pion form factor from the BSE model on-shell ($k_i^2 = m_\pi^2$) and off-shell ($k_i^2 = -1.3 \text{ GeV}^2$) in comparison to the ρ -pole (VDM) and to data [2]

described correctly, but already VDM would have been a nontrivial result as it is not put into the model. The data in the timelike region ($q^2 > 1 \text{ GeV}^2$) are slightly underestimated by our calculations, which do not show a ρ' . In Fig. 4 we have also plotted the off-shell form factor $F_\pi(q, k)$ for a value of $k^2 = -1.3 \text{ GeV}^2/c^2$ where k is the relative momentum between the mesons. Clearly it drops more slowly than the on-shell form factor. This is typical for a field theoretic calculation. Since the theory describes the on-shell pion structure accurately in the spacelike region, we can now confidently try to calculate the pion current contributions given by Fig. 1.

3. The Pion Current

3.1. Basic Formulae

The nucleon form factors are easily extracted from the diagrams of Fig. 1, if the off-shell (with respect to the pions) πN -scattering amplitude is decomposed into the usual A - and B -amplitudes. Convenient combinations of form factors for this projection are $G_M = F_1 + F_2$ and F_2 :

$$G_M(q^2) = \frac{1}{2} Z_N + \frac{1}{3} \int_k |\mathbf{k}| (P_0(z) - P_2(z)) B(p, k) \quad (3.1)$$

$$F_2(q^2) = \frac{1}{1 + \tau_k} \int (i\sqrt{1 + \tau} P_1(z) A(p, k) - |\mathbf{k}| P_2(z) B(p, k)) \quad (3.2)$$

with the following notation (three momenta and angles are in the $N\bar{N}$ -CMS):

$$\left. \begin{aligned} Z_N &= \text{nucleon renormalization constant} \\ p &= \text{nucleon relative momentum} \\ k &= \text{pion relative momentum} \\ k_{1/2} &= q/2 \pm k \\ z &= \cos(\angle(\mathbf{k}, \mathbf{p})) \\ \tau &= -q^2/4M^2, \end{aligned} \right\} \quad (3.3)$$

$$\begin{aligned} \int_k &= -8\pi i \int \frac{d^4 k}{(2\pi)^4} |\mathbf{k}| F_\pi(q, k) A_{\text{eff}}(k_1^2) A_{\text{eff}}(k_2^2) \\ &\Rightarrow -\frac{2i}{\pi^2} \int |\mathbf{k}|^3 d|\mathbf{k}| dk_0 F_\pi(q, k) A_{\text{eff}}(k_1^2) A_{\text{eff}}(k_2^2) \end{aligned} \quad (3.4)$$

after partial wave projection.

Our normalization of A and B is such that the nucleon exchange contribution reads (setting $l = (p - k)^2$):

$$B_N(p, k) = -\frac{2g^2}{4\pi} r_1(l) \Gamma_5(M^2, l, k_1^2) \Gamma_5(M^2, l, k_2^2) \quad (3.5)$$

and

$$A_N(p, k) = -\frac{2g^2}{4\pi} M(r_1(l) - r_2(l)) \cdot \Gamma_5(M^2, l, k_1^2) \Gamma_5(M^2, l, k_2^2), \quad (3.6)$$

where the nucleon propagator is written as

$$\tilde{S}(p) = \not{p} r_1(p^2) + M r_2(p^2). \quad (3.7)$$

In [7] it turned out that for $p^2 < M^2$ (which is the relevant region in (3.4)), one has $r_2(p^2) < r_1(p^2)$. A slightly simplified version of the parametrisation in [7] is

$$M(p^2) \equiv M r_2(p^2)/r_1(p^2) = M/(1 - (p^2 - M^2)/4M^2). \quad (3.8)$$

Consequently the A_N -term (3.6) will give in (3.2) a negative and (since it has no pole) short range contribution to $F_2(q^2)$.

We have not written down the necessary subtractions for (3.1) and (3.2). They are performed at large spacelike momenta of order 10 GeV , so that the bare terms proportional to the renormalization constant Z_N are almost negligible ($Z_N \approx 0.03$). We now shall discuss the results of various approximations to $A(p, k)$ and $B(p, k)$ for the form factors $F_1(q^2)$ and $F_2(q^2)$ and compare them to the experimental values in the region $0 \leq q^2 < -1 \text{ GeV}^2$. For this purpose we regard the dipole formulae

$$\begin{aligned} G_E^p(q^2) &= 1/(1 - q^2/0.71 \text{ GeV}^2/c^2) \\ G_M^p(q^2) &= 2.793 G_E^p(q^2) \\ G_M^N(q^2) &= -1.913 G_E^p(q^2) \\ G_E^N(q^2) &= \tau/(1 + 4\tau) G_E^p(q^2) \end{aligned} \quad (3.9)$$

as valid, since the experimental errors of the neutron form factors [10] are larger than the deviations of the proton form factors from the dipole law [1].

3.2. Nucleon Exchange

In the dispersion analysis [11] the nucleon pole contribution to B plays an important rôle. Similarly we find here that nucleon exchange, (3.5) and (3.6), accounts for almost one half of the anomalous magnetic moment and overestimates the charge. We shall not describe the technical details for the evaluation of the integrals in (3.1) and (3.2). We only remark that, since we are working with complicated analytic forms for the propagator, there remain three nontrivial momentum space integrals which are performed numerically. The singularity in the propagator of the exchanged nucleon forces us, after introduction of hyperspherical coordinates in the $N\bar{N}$ rest system, to deform the momentum integration into the complex plane, the detour depending on q^2 (see [12] for details).

In Table 1, column N we have listed the static values for F_1 and F_2 and for the radii. It is consistent with our reduction of the nucleon box due to π - and Δ -exchange that $F_1(0)$ is quite large. The lowest order contribution [8] to $F_2(0)$ ($\mu'_V = 1.65$) is reduced by more than a factor of 2 by the combined effects of the

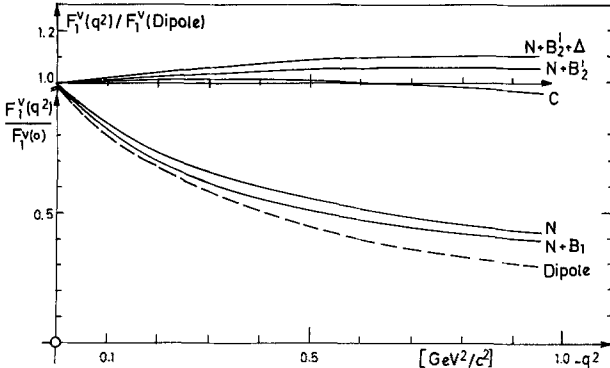


Fig. 5. Results for $F_1^v(q^2)$ in different approximations described in the text. 'Dipole' refers to (3.9)

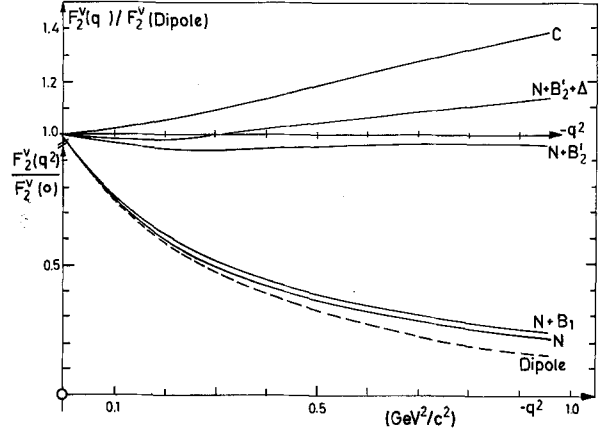


Fig. 6. Results for $F_2^v(q^2)$ in different approximations described in the text. 'Dipole' refers to (3.9)

hadronic vertex Γ_5 and of the A_N -term (3.6). The latter is also important for the q^2 -dependence of $F_2(q^2)$, as it lowers $\langle r_2 \rangle$ by 15% and reduces $F_2(q^2)$ considerably at larger q^2 . We show the results for $F_1(q^2)$ and for $F_2(q^2)$ in Figs. 5 and 6 resp. together with the dipole curves. We find that $F_1(q^2)$ is close to VDM which is a nontrivial result as $F_\pi(q, k)$ differs appreciably from VDM, if the pions are far off-shell. $F_2(q^2)$, if normalized, is actually not far from $F_{2Dipole}$ for $-q^2 < 0.5 \text{ GeV}^2/c^2$ and has an acceptable radius. It falls well below VDM and leads in the timelike region $q^2 > 1 \text{ GeV}^2/c^2$ to a negative imaginary continuum [12].

3.3. $N\bar{N}$ Box with π -Exchange

The diagram of Fig. 1b can be considered as a special case of Fig. 1c. The γ_μ -part of the nucleon vertex, which has been calculated on-shell in the last paragraph and found to be large, is from the lowest order calculation known to be repulsive for the charge,

Table 1.

	exp.		N	$N + B_1$	$N + B_1'$	$N + B_2'$	$N + B_2' + \Delta$	C
$F_1(0)$	1/2		0.905	0.310	0.451	0.717	0.540	0.540
$F_2(0)$	1.85		0.764	1.070	0.747	0.757	1.00	1.694
	Dipole	Proton						
$\langle r_1 \rangle$	0.76	0.80	0.675	0.765	0.770	0.730	0.729	0.758
$[f_m]$		$\pm .02$						
$\langle r_2 \rangle$	0.86	0.92	0.901	0.84	0.920	0.938	0.902	0.831
$[f_m]$		$\pm .02$						

$F_1^v(q^2)$ and $F_2^v(q^2)$: The static values and the radii for experimental and various approximations. Radii are from [1].

N = Nucleon exchange

B = Nucleon + meson exchange (specified in section 3.3 and 3.4)

Δ = Δ exchange

C = $N + B_2' + \Delta + \pi\omega$ -current

but it will increase [8] $F_2(0)$. This we expect to be the dominant character of the box diagram.

In order to calculate the loop, we have decomposed it into A - and B -amplitudes and then partial wave projected with (3.1) and (3.2). The expressions to be inserted into the partial wave projected version of (3.4) are given in appendix B. We concentrate here only on the leading terms given by the S -wave projections of π - and N -exchange which are divergent for point-like couplings. If t is the relative momentum in the loop, we find for the integrand of the t -integral

$$B_B \sim P_0(z)(M^2 - (M - M(\tilde{t}^2))^2 - 1/3 t^2 + t_0^2) Q_{0\pi} Q_{0N} \quad (3.10)$$

where $Q_{0\pi}$ and Q_{0N} are the s -wave projections of π - and N -exchanges in the box. In the nucleon mass term $M(\tilde{t}^2)$ we have replaced the argument by the average momentum of the two opposite nucleon lines. The $r_1(p^2)$ factors are omitted. Similarly we have

$$A_B \sim P_1(z)M(\tilde{t}^2)M|\mathbf{k}| Q_{0\pi} Q_{0N}. \quad (3.11)$$

These two terms are just the dominant part of Fig. 1c, if the $\gamma N \bar{N}$ -vertex is approximated by the γ_μ -coupling given by Fig. 1a.

We now discuss the importance of the various terms in (3.10) and (3.11). In (3.10) M^2 is attractive and of long range with respect to the nucleon loop, whereas the remaining terms are of short range and repulsive. However, for momenta $\tilde{t}^2 \approx 0$ the bracket $(M - M(\tilde{t}^2))^2$ is still small compared to M^2 for the parametrisation (3.8), so this term is not important. The A_B expression (3.11) is a positive contribution to F_2 , which is well convergent with respect to t , since its short range part is suppressed by the decreasing $M(\tilde{t}^2)$.

The same remarks as in (3.2) hold for the t integrals of the nucleon loop, but the contour deformation extends much farther into the complex t -plane. In column " $N + B_1$ " of Table 1 we combine the results from this diagram with those from N -exchange. One sees a drastic reduction of $F_1(0)$ and considerable improvement in $\langle r_1 \rangle$. On the other hand $F_2(0)$ is increased and $\langle r_2 \rangle$ lowered, such that it no longer agrees with the measurements of $\langle r_2 \rangle$ for the proton alone. This is not unexpected, since the high intermediate masses of the loop will not lead to a rapid q^2 -fall-off, and one sees the influence of the too flat $F_1(q^2)$ as given by Fig. 1a (see Fig. 5, curve N).

The mass terms $M(\tilde{t}^2)$ have to be discussed further, since higher order corrections probably cannot be neglected for them. The mass term of a nucleon line between two mesons in the isospin 0 state receives large negative contributions from meson exchange as shown in Fig. 7, their magnitude being roughly three times that of the repulsive B -term. This fact was already explained and used in the determination of the nucleon propagator [7]. The isospin decomposition of fig. 1b gives $(0; 1) + (1; 0) - (1; 1)$, where the

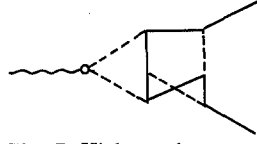


Fig. 7. Higher order corrections especially for mass term $M(p^2)$

two numbers in the bracket indicate the I -spin of the pion pairs on the r.h.s. and l.h.s. of fig. 1b resp. Therefore the repulsive force in the $I=0$ state will dominate. Tentatively we use the same suppression factor for the mass term as in [7], namely

$$M(p^2) = M/(1 - (p^2 - M^2)/M^2). \quad (3.13)$$

It is amusing to note that the suppression at $p^2 = 0$ agrees with that given by the contact interaction of the chiral invariant Lagrangian of Gürsey [13]. If we would apply (3.13) to on-shell πN -scattering at threshold, we would obtain twice the A^+ -term following from Adlers selfconsistency condition [14].

The form (3.13) clearly will reduce the A -term in (3.11). As can be seen in column $N + B_1$ in Table 1, the effect is so strong that for $F_2(0)$ the nonleading terms become important. The decrease of the A -term will of course lead to an increase of the charge $F_1(0)$. The q^2 -dependence of $F_2(q^2)$ is improved drastically and the value for $\langle r_2 \rangle$ is in excellent agreement with experiment. We do not show the curves for $F_1(q^2)$ and $F_2(q^2)$ in Figs. 5 and 6, since they are very similar to those obtained in the approximation with ω - and ε -exchange in the nucleon box. These will be discussed in the next chapter.

3.4. $N \bar{N}$ -Box with ω - and ε -Exchange

The reduction of $F_1(0)$ due to π -exchange is certainly overestimated, as it is generally true for the Born term of a repulsive potential. Especially after Δ -exchange is included, $F_1(0)$ is quite low. One therefore should include multi-meson exchange diagrams which compensate part of the repulsive π -exchange. We want to avoid this, however, because of the spin complications and consider only ω - and ε -meson exchanges. For the coupling constants we shall use $g_{\omega N \bar{N}}^2/4\pi = 15$ which can be justified from our simplified model of Appendix A. The coupling $g_{\varepsilon N \bar{N}}$ is poorly defined as is the ε -particle itself. At the moment we choose $g_{\varepsilon N \bar{N}} = g_{\omega N \bar{N}}$ and justify this a posteriori by the charge normalization.

Again we shall work with free propagators for the reasons explained in Sect. 2.3. (note that single pion exchange as part of the ω -propagator is forbidden and double exchange is already included).

The formulae for the partial wave projected integrals are collected in appendix B. Essentially the same remarks as in the previous subsection apply for ε - and ω -exchange with the difference that the F_1 -projection is attractive and that a suppression

of the $M(p^2)$ -term will cut out a short range attractive piece.

For the chosen values of coupling constants and for the mass term (3.13) we find $\Delta F_1(0) = 0.27$ (see Table 1, column $N + B'_2$). The q^2 -dependence for both form factors is quite good (see Figs. 5 and 6). For the mass term (3.8) the form factor $F_2(q^2)$ is much too high at $q^2 = -1 \text{ GeV}^2/c^2$. It is mainly the A -term with its slowly converging k -integration which causes this difficulty.

The elimination of the "hard component" by modifying the mass term is not the only correction which we have to apply. We have to be aware that the lowest order loop for $F_1(q^2)$, Fig. 1a is a poor approximation which is improved by the box diagrams independently of the mass term. Thus the $F_2(q^2)$ part of the boxes will get corrections in higher order ladder exchanges between the nucleons, which we shall not attempt to calculate here. In general we regard the phenomenological parametrization of $M(p^2)$ for the isoscalar πN -amplitude as a promising step towards a realistic model.

3.5. $\Delta(1232)$ -Exchange

Simple charge counting suggests that Δ -exchange gives a negative contribution to $F_1(0)$. The notion of Δ -exchange is certainly model dependent, but as the explanation of the Δ as a πN resonance generated by N exchange is a fairly successful theory [15], we can define Δ -exchange as the sum of πN ladder diagrams, the simplest nontrivial of which is the $N\bar{N}$ box diagram Fig. 1b. We adopt the treatment from on-shell πN -scattering [17], where the Δ -pole terms for the A - and B -terms are known to be a good approximation for the dispersion integrals. These pole terms can conveniently be calculated from the Rarita-Schwinger propagator [16]. We find ($\Delta = \Delta$ -mass, $\delta = \Delta^2 - M^2$)

$$A_\Delta = \frac{2g^{*2}}{3} \frac{1}{4\pi} \frac{1}{(p-k)^2 - \Delta^2} \left\{ (M + \Delta)(k^2 - \frac{9^2}{4} - \delta/3 - \frac{1}{6\Delta^2}(\delta + k_1^2)(\delta + k_2^2)) + \frac{1}{6\Delta}(\delta^2 - k_1^2 k_2^2) \right\} \quad (3.14)$$

$$B_\Delta = \frac{2g^{*2}}{3} \frac{1}{4\pi} \frac{1}{(p-k)^2 - \Delta^2} \left\{ \frac{k^2}{3} - \frac{5}{12}q^2 + M^2 + \frac{M}{3\Delta}(\Delta^2 + M^2) - \frac{1}{6\Delta^2}(\Delta^4 + M^4) - \frac{1}{3\Delta^2}(\Delta M - M^2) \left(k^2 + \frac{q^2}{4} \right) - \frac{1}{6\Delta^2} k_1^2 k_2^2 \right\} \quad (3.15)$$

We use $g^{*2}/4\pi = 0.26/m_\pi^2$ according to [17]. The above pole terms we corrected first of all by the vertex functions Γ_5 in the same way as the nucleon pole in (3.5). The justification for this is that the $\pi N \Delta$ coupling arises through the πN coupling in the nucleon exchange loops. Secondly we multiply A_Δ

and B_Δ by the vertex function (depending only on k_1^2 or k_2^2) which has been found in the study of the $\gamma N \Delta$ vertex as a function of the photon momentum squared in [15]. It is

$$\Gamma_\Delta(k^2) = 1/(1 - (k^2 - m_\pi^2)/3M^2). \quad (3.16)$$

This vertex, which is a special consequence of the P -wave state in the πN channel makes the Δ -contribution convergent. We shall work with the free Δ -propagator for similar reasons as we did for the ω -propagator. Here it is the box diagram Fig. 1b, which probably has the slowest fall-off in $(p-k)^2$ and which has to be omitted from the πN -scattering amplitude, as it is already included.

In Table 1 we see a substantial decrease of $F_1(0)$ and an increase of $F_2(0)$ with slight changes in the radii. A change in the cut-off in (3.16) from $3M^2$ to $2M^2$ would increase $F_1(0)$ by 10% and $F_2(0)$ by -5%. The q^2 -behaviour of both form factors is quite good, with a tendency to be high at large q^2 for $F_2(q^2)$ (see Figs. 5 and 6). Of course this description cannot be the final one, as the normalization of $F_2(0)$ is still very low. This will be cured by the $\pi\omega$ -current (Fig. 2), which on the other hand will bring difficulties at high q^2 .

4. The $\pi\omega$ -current

We shall treat the $\pi\omega$ -intermediate state only in the one nucleon exchange approximation of Fig. 2, i.e. we especially neglect meson exchanges between $N\bar{N}$. The $\pi\omega\gamma$ form factor $F_{\pi\omega\gamma}(q^2)$ follows from the coupled channel BSE with nucleon loops as described in GW. The projection of the diagram Fig. 2 is, assuming as always a pure γ_μ -coupling between ω and $N\bar{N}$:

$$G_M(q^2) = -\frac{M}{3} \int_k (2P_0(z) + P_2(z)) r_1((p-k)^2) \quad (4.1)$$

$$F_2(q^2) = G_M(q^2) + \frac{2M\tau}{1+\tau} \int_k P_2(z) r_1((p-k)^2) \quad (4.2)$$

The notation is the same as in (3.3) except for

$$\int_k = 2g g_{\omega N\bar{N}} \int \frac{d^4 k}{i(2\pi)^4} |\mathbf{k}|^2 F_{\pi\omega\gamma}(q, k) \tilde{\Delta}_\pi(k_1^2) \Delta_\omega(k_2^2) \quad (4.3)$$

where again the free ω -propagator is used. For simplicity we have neglected the difference $r_1(p^2) - r_2(p^2)$ here since it would show up only in P -waves. There is a subtlety for the choice of the coupling constant $g_{\omega N\bar{N}}$ in (4.3) as compared to the one which is used for the $\pi\pi \rightarrow \pi\omega$ nucleon loop. We have argued in GW that the inclusion of the crossed nucleon box will increase the effective $\omega N\bar{N}$ coupling by a factor of 2. We therefore take in (4.3) only half of that value, which was determined by adjusting $F_{\pi\omega\gamma}(0)$. This leads to a lower value than that used for ω -exchange between $N\bar{N}$, namely

$$g_{\omega N\bar{N}}^2/4\pi = 8.6. \quad (4.4)$$

From (4.1) and (4.2) we recognize that especially for $F_2(q^2)$ the k -integral behaves quite different from the pion current case: There is a S -wave projection of the nucleon propagator $r_1((p-k)^2)$ which would be logarithmically divergent for a pointlike vertex $F_{\pi\omega\gamma}(q,k)$. Although $F_{\pi\omega\gamma}$ is not pointlike since it arises from convergent fermion loops, its decrease in momentum space is not strong enough to make the integral (4.1) converge as quickly as the corresponding pion integral (3.2). The large ω -mass will work in the same direction. It is therefore not surprising that the inclusion of the $\pi\omega$ -current lowers the radius for F_2 considerably (last column of Table 1, version C). Furthermore the q^2 -dependence is no longer compatible with the dipole behaviour (see Fig. 6). On the other hand, the contribution to $F_1(q^2)$ (which vanishes for $q^2=0$), leads to a 15% decrease at $q^2 = -1 \text{ GeV}^2/c^2$, so that $F_1(q^2)$ is already somewhat low there (see Fig. 5). The radius $\langle r_1 \rangle$, which depends only on $F_{\pi\omega\gamma}(0)$, is in very good agreement with experiment.

The most likely source of this discrepancy is the behaviour of $F_{\pi\omega\gamma}(q^2)$ in our model. It drops less rapidly with q^2 than VDM. Perhaps the $F_{\pi\omega\gamma}$ -form factor can be changed in our model. Preliminary calculations indicate, that the introduction of an attractive ($\pi\omega \rightarrow \pi\omega$)-interaction will lead to a stronger decrease with q^2 . This force can be derived from the nucleon loop [18] and was neglected in GW. It may eventually lead to a second resonance in the $\pi\omega$ channel, which one naturally expects for a many channel problem with attractive potentials.

We conclude that the size of the $\pi\omega$ -current at $q^2=0$ is reasonable as the normalization of $F_2(0)$ and the radius of F_1 suggest. The k -integral for F_2 however, has a tail extending to rather high k^2 , and the $F_{\pi\omega\gamma}$ -vertex is neither sufficiently soft in k^2 nor in q^2 . The overall result is nevertheless in surprising agreement with experiment in view of the fact that in our model the nucleon form factors don't contain any free parameters.

5. Discussion

Let us repeat our basic assumptions. We believe that vector mesons can be described as resonances in a multichannel system made up by $\pi\pi$, $K\bar{K}$, $\pi\omega$, $N\bar{N}$ channels and by those physical states which build up the selfenergy continuum in the propagators of these particles. The main forces in the isovector case are nucleon exchange for $N\bar{N} \rightarrow \pi\pi$ and $N\bar{N} \rightarrow \pi\omega$, and in the isoscalar case pion exchange between $N\bar{N}$. The most important parameter is the vertex scale parameter Λ , which is fixed by the ρ mass.

A necessary consistency check is first of all, that the couplings of the various constituents to the vector mesons are described correctly. These include the ρ -width, which is typically high by 30% if we do not adopt some modifications (which is already a good result). Furthermore we have the $\rho\pi\omega$ coupling or

$F_{\pi\omega\gamma}$ which can be reproduced by a reasonable value for $g_{\omega N\bar{N}}$. The couplings of the ρ to $N\bar{N}$ follow from the form factor normalizations and the e.m. radii as calculated in this paper.

The second test concerns the 'spatial' properties of the particles, i.e. the higher q^2 -behaviour of the form factors. In detail our calculations give the following picture:

The normalization of the anomalous isovector moment is partly shifted from the pure loop diagram [8] to higher order contributions, namely to the $\pi\omega$ -current and to Δ -exchange. The reduction of the pion current is due to the hadronic vertex functions, the A -term according to (3.6) and to the mass suppression (3.13) in the nucleon boxes. There is some uncertainty for the precise values of these higher order terms, since e.g. the $\omega N\bar{N}$ coupling constant and the ω -propagator are not well known. They can, however, be calculated in our model, as we have shown in a simplified BSE-calculation.

The charge normalization is fulfilled via a large contribution from nucleon exchange for the pion current, further positive terms from ω - and ε -exchange and negative currents from π - and Δ -exchange. We remark that in principle the uncertainty in the ω - and ε -exchanges will not fully enter into $F_1(0)$, as it will also influence the nucleon loop and the value of Λ^2 necessary to reproduce the correct ρ -mass. On the other hand $F_1(0)$ depends strongly on Λ^2 .

The two isovector radii are generally quite good for all calculated contributions. In detail the nucleon exchange term for $F_1(q^2)$ has a long tail in momentum space, which gives a low value for $\langle r_1 \rangle$. This result is readily corrected by the other diagrams. Except for the $\pi\omega$ -current and for the boxes with unmodified mass term, there is a tendency for $\langle r_2 \rangle$ to lie above the dipole values in agreement with the low q^2 -measurements from Mainz [1].

Whereas the final version C for $F_1(q^2)$ describes the experimental results very well, there are definite difficulties for $F_2(q^2)$ at increasing q^2 , with deviations up to 35% at $q^2 = -1 \text{ GeV}^2/c^2$. This is due to the $\pi\omega$ -current. Since it is possible to extend this model into the timelike region [12], it will be possible to check the crucial $\pi\omega$ -form factor against the data for $e^+e^- \rightarrow \pi\omega$. A simplified version of our model shows no ρ' below 2 GeV. Whether this can be changed by the inclusion of more elastic forces like direct $\pi\omega \rightarrow \pi\omega$ couplings will be explored in the future.

It is surprising that a field theoretic model with not superrenormalizable interactions and a vertex scale parameter $\Lambda^2 \approx 2 \text{ GeV}^2$ (the influence of which is counterbalanced by the propagator modifications) can lead to the correct magnetic moment radius and to a form factor decrease with q^2 definitely faster than a monopole. Although the position of the ρ -pole is an essential input parameter for the model, it is not trivial that the model first of all shows approximate vector dominance and secondly gives deviations

from VDM of the correct sign and, approximately, of the correct magnitude. It is intuitively clear that in a field theoretic model the form factor decrease for high q^2 does not come out in an easy way, since the lowest order contributions are pointlike for the charge and nearly pointlike [3] for $F_2(q^2)$. The ad hoc multiplication of the lowest order loops with the on-shell pion form factor [19] still does not give satisfactory results [12] and it is hard to justify, as the off-shell pion form factor deviates considerably from the on-shell values. Furthermore a model with a limited number of channels is likely to possess a small number of vector mesons, perhaps only one [12] as the consequence of our singular interactions. These arguments make it understandable that the theory approaches the final result from above. This is in striking contrast to the approach in the quark model, where one is led, by the observation of linear Regge trajectories, to smooth potentials between the constituents [20], which guarantees a rapid decrease of the form factors for $q^2 \rightarrow \infty$.

Usually in constituent models the wave function of the constituents is the quantity of prime interest, whereas the form factor of the constituents attracts little attention. Here we suffer somewhat from the opposite danger. The wave function is (apart from the particle propagators) given by our vertex function Γ_5 , the form of which is guessed with only its scale parameter determined. Since, however, the scale of 2 GeV² is relatively large, it may be that for our small region of q^2 we do not probe the details of this function. Nevertheless a better understanding of the basic vertex and of some other important dynamical input amplitudes, like e.g. the isoscalar mass term, are urgently needed.

Appendix A

Here we want to study both the form of the ω -propagator and the effects of higher order meson exchange insertions in the nucleon loop for $\pi\pi$ -scattering. For both purposes we shall solve the $N\bar{N}$ -BSE in the spin-1 channel, handling the spin problem only approximately. As forces we shall consider π -, ω - and ε -exchange.

A.1. $N\bar{N}$ -Scattering, Isoscalar Case

We shall investigate how well the scattering amplitude for off-shell nucleons with momenta p^2 in the range $0 > p^2 > -M^2$ is dominated by the ω -pole with a γ_μ -coupling, if the forces are given by meson exchanges. First we have to simplify the spin problem. The dominant π -exchange amplitude $\gamma_5 \otimes \gamma_5$ can be decomposed by the Fierz transformation into $-1/4 \gamma^\mu \otimes \gamma_\mu$ and other terms, where γ_μ now acts between $N\bar{N}$ -spinors. This γ_μ we take as the spin part of the inhomogeneous term of the BSE. Then it

reads for π exchange

$$T_\mu(p) = -\frac{3}{4} \frac{g^2}{4\pi} \gamma^\mu \frac{1}{(p-p')^2 - m_\pi^2} - 3g^2 i \int \frac{d^4 k}{(2\pi)^4} \gamma_5 (k_1 + M) T_\mu(k) (k_2 + M) \gamma_5 / (k_1^2 - M^2)(k_2^2 - M^2)((k-p)^2 - m_\pi^2) \quad (\text{A1})$$

with $k_{1/2} = \pm q/2 + k$

We now proceed as if we could integrate symmetrically with respect to k . This is exact for $p = q = 0$ and for $k \rightarrow \infty$ (Note that we are not interested in $T_\mu(p)$ for $p^2 \sim M^2$, where symmetric integration is rather poor. This region is not important for the ω -exchange in the BS-kernel). Since we are interested into the q^2 -dependence, we cannot neglect the anomalous magnetic moment terms, which arise from the combination

$$M \left(\frac{\not{q}}{2} \gamma_\mu - \gamma_\mu \frac{\not{q}}{2} \right)$$

in (A1). We are therefore led to a system of coupled integral equations, if we introduce two form factors by

$$T_\mu(p) = \gamma_\mu F_1(p) + \frac{1}{2} [\not{q}, \gamma_\mu] F_2(p), \quad (\text{A2})$$

$$F_1(p) = -\frac{3}{4} \frac{g^2}{4\pi} Q_0(p) - c_\pi \int_k \left(M^2 + \frac{q^2}{4} - \frac{k^2}{2} \right) F_1(k) + q^2 M F_2(k), \quad (\text{A3})$$

$$F_2(p) = c_\pi \int_k M F_1(k) + \left(M^2 + \frac{q^2}{4} \right) F_2(k), \quad (\text{A4})$$

$Q_0(p)$ = S -wave projection of pion propagator with final relative momentum p

$$c_\pi = \frac{3g^2}{4\pi}$$

$$\int_k = -\frac{i}{\pi^2} \int d k_0 d|\mathbf{k}| \mathbf{k}^2 Q_0(p, k) / (k_1^2 - M^2)(k_2^2 - M^2). \quad (\text{A5})$$

It should be noted that the second order contribution to F_1 via the F_2 -amplitude is linear in q^2 and gives rise to a strong q^2 -variation.

We also give the equations for ω - and ε -exchange:

$$F_1(p) = -\frac{1}{2} \frac{g_{\omega N\bar{N}}^2}{4\pi} Q_0(p) - 2c_\omega \int_k \left(M^2 + \frac{q^2}{4} - \frac{k^2}{2} \right) F_1(k) \quad (\text{A6})$$

$$F_2(p) = 0 \quad (\text{A7})$$

and

$$F_1(p) = -\frac{1}{4} \frac{g_{\varepsilon N\bar{N}}^2}{4\pi} Q_0(p) - c_\varepsilon \int_k \left(M^2 + \frac{q^2}{4} - \frac{k^2}{2} \right) F_1(k) + q^2 M F_2(k) \quad (\text{A8})$$

$$F_2(p) = -c_\varepsilon \int_k M F_1(k) + \left(M^2 + \frac{q^2}{4} \right) F_2(k) \quad (\text{A9})$$

with $c_\omega = g_{\omega N\bar{N}}^2/4\pi$ and $c_\varepsilon = g_{\varepsilon N\bar{N}}^2/4\pi$. Note the different sign of the F_2 -integral as compared to π -exchange. The modifications due to dressing the propagators are straightforward. For simplicity we set $M \rightarrow M(k^2 + q^2/4)$.

We have solved the coupled equations with the choice $g_{\omega N\bar{N}} = g_{\varepsilon N\bar{N}} = g$ with $g^2/4\pi$ left as parameter. The value for $g_{\omega N\bar{N}}$ will be determined selfconsistently in the course of this calculation and is not far from the above choice. The choice for $g_{\varepsilon N\bar{N}}$ is motivated by the correct charge normalization for F_1 as explained in Sect. 3.4. Because of the large isospin factor and the small mass, pion exchange is still the dominant force. We obtain a bound state at the mass $q^2 = m_\omega^2$ for the value $g^2/4\pi = 14.9$, which gives credibility to our model. We now can examine the resulting $N\bar{N}$ -scattering amplitude F_1 without the inhomogeneous term (see Sect. 2.3) for various external momenta p^2 , which we take as equal. In Fig. 8 we have plotted (as solid lines) the function

$$(q^2 - m_\omega^2) F_1(q^2, p^2) / \Gamma_5^2(p^2, p^2, q^2) \quad (\text{A10})$$

for three values of p^2 . The dashed lines are obtained, if also the second order diagram is omitted. If the expression (A10) were a constant, we could identify it with the coupling constant $g_{\omega N\bar{N}}^2/4\pi$. We see a variation up to 20% with q^2 and a decrease by a factor of 2 with increasing $|p^2|$. If the second order is subtracted, the q^2 -dependence is negligible. This means that $F_1(p^2, q^2)$ decreases somewhat faster than the pseudoscalar vertex function Γ_5 which is not surprising in view of the long range forces due to pion exchange.

For the value of the coupling constant $g_{\omega N\bar{N}}^2/4\pi$ one finds an average between 15 and 20 depending on p^2 and the subtractions. This is an overestimation, since we have neglected all annihilation channels. The value of 15 is therefore a very reasonable estimate.

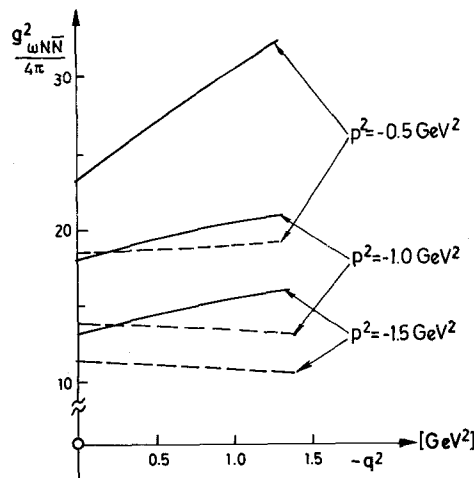


Fig. 8. Effective coupling constant $g_{\omega N\bar{N}}^2/4\pi$ as function of p^2 and q^2

In a first order approximation the decreasing vertex (as function of p^2) will be counteracted by the increase of the propagator in q^2 relative to the free one, and we can take the product of our vertex function Γ_5 and the free propagator as a good working hypothesis for the off-shell $N\bar{N}$ scattering amplitude. Possible deviations have to be studied in more detail in the complete model [9].

A.2. The Nucleon Box for $\pi\pi$ -Scattering

The approximation discussed above enables us to calculate also meson exchange corrections for the nucleon loop, which is the dominant force in the $\pi\pi$ -channel. We only have to change the inhomogeneous term and the π -exchange isospin factor. First of all the nucleon exchange diagram for the amplitude $\pi\pi \rightarrow N\bar{N}$ gives, if contracted with the pion e.m. vertex, a γ_μ -current proportional to $2g^2 Q_0(p-p')$ (p' refers to pion momenta, Q_0 is the s -wave projection of the nucleon propagator). Then we introduce form factors in analogy to (A2) and find the equations

$$F_1(p) = 2g^2 Q_0(p-p') - c'_\pi \int_k \left(M^2 + \frac{q^2}{4} - \frac{k^2}{2} \right) F_1(k) + q^2 F_2(k) \quad (\text{A11})$$

$$F_2(p) = c'_\pi \int_k M F_1(k) + \left(M^2 + \frac{q^2}{4} \right) F_2(k) \quad (\text{A12})$$

with

$$c'_\pi = -g^2/4\pi.$$

The ω - and ε -exchange terms are unaltered. The complete p -wave projection of the box (with respect to the pions) will be obtained from the solution of (A11) and (A12) by adding the second nucleon exchange:

$$T_{\text{Box}} = 2c'_\pi \int_{k_N} \left(M^2 + \frac{q^2}{4} - \frac{k^2}{2} \right) F_1(k) + q^2 F_2(k) \quad (\text{A13})$$

Here \int_{k_N} refers to N -exchange.

Solving these equations by iteration leads to the following results: If we neglect ω - and ε -exchange, the box diagram is reduced by about 20%, which is somewhat less than speculated in GW. If we include ω - and ε -exchange, we find an enhancement of 10% relative to the 'bare' box and an additional q^2 -dependence, which is almost linear and gives a variation of +9% between $q^2 = 0$ and $q^2 = m_\rho^2$. All this qualitatively agrees with the exact results of Chan [9]. Since we have neglected Δ -exchange, which reduces the isovector charge by 20% (see Table 1), a certain reduction of the nucleon box will survive the net attraction of meson exchanges.

In order to obtain the correct ρ -width, we also have speculatively increased the energy dependence of the box from 9 to 15%. This energy dependence

however has to be damped for large off-shell momenta of the external pions, as then the internal momenta in the loops (e.g. the term $-k^2/2$ in the kernel of (A11)) become larger. We therefore use the following form for the effective $\pi\pi$ -kernel, $\tilde{T}_{\text{Box}}(k_i)$, where k_i are the pion momenta:

$$\begin{aligned} & \tilde{T}_{\text{Box}}(k_i) \\ &= 0.8 \left\{ 1 + 0.15 q^2/m_\rho^2 \left(1 - \sum_{i=1}^4 k_i^2/40M^2 \right) \right\} T_{\text{Box}}(k_i) \end{aligned} \quad (\text{A14})$$

$T_{\text{Box}}(k_i)$ is the unmodified pseudoscalar Box diagram [6]. In conclusion we see that meson exchange corrections in the nucleon loop are not very large in contrast to the isoscalar case. The reason for this is the cancellation between attractive and repulsive forces.

Appendix B

Here we collect the contributions to $G_M(q^2)$ and $F_2(q^2)$ which arise from the meson exchange box diagram of Fig. 1b. These can be viewed as corrections to the nucleon exchange amplitude for $\pi\pi \rightarrow N\bar{N}$. We have decomposed the spin part of this amplitude into the familiar A - and B -parts with the help of the algebraic program REDUCE [21]. Then the partial wave projection was done with (3.1) and (3.2). The D -wave exchange was neglected in order to simplify the formulae. Besides the definition of \int_k from (3.4) we use the abbreviations

$$\int_k = \frac{-i}{\pi^2} \int t^2 d|t| dt_0 r_1 \left(\left(\frac{q}{2} + t \right)^2 \right) r_1 \left(\left(\frac{q}{2} - t \right)^2 \right)$$

$$C_t = M_t^2 - \frac{q^2}{4} - t + 2k_0 t_0$$

$$M_t = M \left(t^2 + \frac{q^2}{4} \right).$$

Then we have for π -exchange:

$$\begin{aligned} G_M(q^2) &= \frac{1}{3} \lambda_\pi \int_k \int_t (Q_{0\pi} - Q_{2\pi}) \left(\frac{2}{3} |\mathbf{k}| |\mathbf{t}| Q_{0N} - C_t Q_{1N} \right) \\ &+ 2 |\mathbf{k}| |\mathbf{t}| |\mathbf{q}| Q_{1\pi} Q_{0N} \\ &+ |\mathbf{k}| \left(2MM_t - M^2 - \frac{q^2}{4} + t^2 \right) Q_{0\pi} Q_{0N} \end{aligned}$$

$$\begin{aligned} F_2(q^2) &= \frac{\lambda_\pi}{1 + \tau_{k t}} \int_k \int_t |C_t| Q_{2\pi} Q_{1N} \\ &+ \frac{2}{3} |\mathbf{k}| (|\mathbf{q}| |\mathbf{t}| Q_{1\pi} - t^2 Q_{2\pi}) Q_{0N} \\ &- M_t/M (|\mathbf{q}| C_t Q_{1\pi} Q_{1N} - \frac{2}{3} |\mathbf{k}| |\mathbf{q}| |\mathbf{t}| Q_{1\pi} Q_{0N}) \\ &+ \frac{2}{3} |\mathbf{k}| q^2 Q_{0\pi} Q_{0N} \end{aligned}$$

$$\lambda_\pi = 4 \left(\frac{g^2}{4\pi} \right)^2$$

ω -exchange:

$$G_M(q^2) = \frac{\lambda_\omega}{3} \int_k \int_t (Q_{0\omega} - Q_{2\omega}) (|t| C_t Q_{1N} - \frac{2}{3} |\mathbf{k}| t^2 Q_{0N})$$

$$+ |\mathbf{k}| \left(2|\mathbf{t}| |\mathbf{q}| Q_{1\omega} + \left(M_t^2 + \frac{q^2}{4} - t^2 \right) Q_{0\omega} \right) Q_{0N},$$

$$\begin{aligned} F_2(q^2) &= \frac{\lambda_\omega}{1 + \tau_{k t}} \int_k \int_t |C_t| Q_{2\omega} Q_{1N} \\ &+ \frac{2}{3} |\mathbf{k}| |\mathbf{q}| |\mathbf{t}| (2M_t/M - 1) Q_{1\omega} Q_{0N} \\ &- \frac{2}{3} |\mathbf{k}| t^2 Q_{2\omega} Q_{0N} - 2|\mathbf{q}| M_t/M C_t Q_{1\omega} Q_{1N}, \\ \lambda_\omega &= 4g_{\omega N\bar{N}}^2 g^2 / (4\pi)^2 \end{aligned}$$

ε -exchange:

$$\begin{aligned} G_M(q^2) &= \frac{\lambda_\varepsilon}{3} \int_k \int_t (Q_{0\varepsilon} - Q_{2\varepsilon}) (|t| C_t Q_{1N} - \frac{2}{3} |\mathbf{k}| t^2 Q_{0N}) \\ &- |\mathbf{k}| \left(2|\mathbf{t}| |\mathbf{q}| Q_{1\varepsilon} - \left(M_t^2 + 2M_t M + \frac{q^2}{4} - t^2 \right) Q_{0\varepsilon} \right) Q_{0N}, \end{aligned}$$

$$\begin{aligned} F_2(q^2) &= \frac{\lambda_\varepsilon}{1 + \tau_{k t}} \int_k \int_t |C_t| Q_{2\varepsilon} Q_{1N} \\ &- \frac{2}{3} |\mathbf{k}| |\mathbf{q}| |\mathbf{t}| (M_t/M - 1) Q_{1\varepsilon} Q_{0N} \\ &- \frac{2}{3} |\mathbf{k}| t^2 Q_{2\varepsilon} Q_{0N} + \frac{M_t}{M} \left(\frac{2}{3} |\mathbf{k}| q^2 Q_{0\varepsilon} Q_{0N} + |\mathbf{q}| Q_{1\varepsilon} Q_{1N} \right), \end{aligned}$$

$$\lambda_\varepsilon = 2g_{\varepsilon N\bar{N}}^2 g^2 / (4\pi)^2$$

The necessary subtractions are straightforward, and we do not list the formulae.

References

- Borkowski, F., Simon, G.G., Walther, V.H., Wendling, R.D.: Nucl. Phys. **B93**, 461 (1975) and references quoted therein
- Bebek, C.J. et al.: Phys. Rev. **D17**, 1963 (1978) (Cornell)
- Brown, C.N. et al.: Phys. Rev. **D8**, 92 (1973) (CEA)
- Brauel, P. et al.: Phys. Letters **69B**, 253 (1977) (DESY)
- Chew, G.F., Karplus, R., Gasiorowicz, S., Zachariasen, F.: Phys. Rev. **110**, 265 (1958)
- Federbusch, P., Goldberger, M.L., Treiman, S.B.: Phys. Rev. **112**, 642 (1958)
- Yoh, J.K. et al.: Phys. Rev. Lett. **41**, 684 (1978)
- Field, R.D. Phys. Rev. Lett. **40**, 997 (1978)
- Gutbrod, F. Phys. Rev. **D6**, 3631 (1972)
- Gutbrod, F., Weiss, U.: Nucl. Phys. **B90**, 52 (1975)
- Gutbrod, F.: DESY 78/65 (to be published)
- Fried, B.D.: Phys. Rev. **88**, 1142 (1952)
- Chak Wing Chan: Internal Report DESY T-78/03 (1978)
- Felst, R.: DESY 73/56
- Frazer, W.R., Fulco, J.R.: Phys. Rev. **117**, 1609 (1960)
- Höhler, G.: In Current induced reactions. Lecture Notes in Physics **56**, p. 159 Berlin, Heidelberg, New York: Springer 1976
- Willrodt, J.: Nucl. Phys. **B116**, 118 (1976)
- Hartmann, G.: Internal Report DESY T-78/02 (1978)
- Gürsey, F.: Nuovo Cimento **16**, 230 (1960)
- Adler, S.L.: Phys. Rev. **137B**, 1022 (1965)
- Gutbrod, F.: DESY 69/33 (unpublished)
- Tjon, J.A., Nieland, H.M.: In: The Padé approximant in theoretical physics, Baker, G.A. jr., Gammel, J.L. eds New York: Academic Press, 1970
- Rarita, W., Schwinger, J.: Phys. Rev. **60**, 61 (1941)
- Höhler, G., Jakob, H.P., Strauss, R.: Nucl. Phys. **B39**, 237 (1972)
- Chak Wing Chan: Private communication
- Beg, M.A.B., Bernstein, J., Tausner, J.: Phys. Rev. **173**, 1523 (1968)
- Feynman, R.P., Kislinger, M., Ravndal, F.: Phys. Rev. **D3**, 2706 (1971)
- Reduce-Manual: Hearn, A.C., Stanford Report CS-70-181